# *Integrative and Conjugative Elements (ICEs): What They Do and How They Work*



**Citation:** Johnson, Christopher M., and Alan D. Grossman. "Integrative and Conjugative Elements (ICEs): What They Do and How They Work." Annual Review of Genetics 49.1 (2015): 577–601.

**As Published:** http://dx.doi.org/10.1146/annurev-genet-112414-055018

**Publisher:** Annual Reviews

**Persistent URL:** http://hdl.handle.net/1721.1/107728

**Version:** Author's final manuscript: final author's manuscript post peer review, without publisher's formatting or copy editing

# Critical components of the conjugation machinery of the integrative and conjugative element ICE*Bs1* of *Bacillus subtilis*

Running title: Conjugation machinery of ICE*Bs1*

Cori T. Leonetti[1*], Matt A. Hamada[1*], Stephanie J. Laurer[1*], Matthew P. Broulidakis[1], Kyle J. Swerdlow[1], Catherine A. Lee[2], Alan D. Grossman[2], and Melanie B. Berkmen[1#]

[1]Department of Chemistry and Biochemistry; Suffolk University; Boston, MA 02114

[2]Department of Biology; Massachusetts Institute of Technology; Cambridge, MA 02139

[*] Co-first authors.

# Correspondence to:

Melanie B. Berkmen

Department of Chemistry and Biochemistry

Suffolk University

41 Temple St.

Boston, MA 02114

phone: 617-921-0654

email: mberkmen@suffolk.edu

## ABSTRACT

Conjugation, or mating, plays a profound role in bacterial evolution by spreading genes that allow bacteria to adapt to and colonize new niches. ICE*Bs1*, an integrative and conjugative element of *Bacillus subtilis*, can transfer itself and mobilize resident plasmids. DNA transfer is mediated by a Type IV secretion system (T4SS). Characterized components of the ICE*Bs1* T4SS include the conserved VirB4-like ATPase ConE, a bifunctional cell wall hydrolase CwlT, and the presumed VirD4-like coupling protein ConQ. Previously, we showed that a fusion of ConE to green fluorescent protein (GFP) localizes to the membrane preferentially at the cell poles. One or more ICE*Bs1* proteins are required for ConE's localization at the membrane, as ConE lacks predicted transmembrane segments and ConE-GFP was found dispersed throughout the cytoplasm in cells lacking ICE*Bs1*. Here we analyzed five ICE*Bs1* genes to determine if they are required for DNA transfer and/or ConE-GFP localization. We found that *conB*, *conC*, *conD*, and *conG,* but not *yddF,* are required for both ICE*Bs1* transfer and plasmid mobilization. All four required genes encode predicted integral membrane proteins. *conB,* and to some extent *conD,* were required for localization of ConE-GFP to the membrane. Using an adenylate cyclase-based bacterial two-hybrid system, we found that ConE interacts with ConB. We propose a model in which the ICE*Bs1* conjugation machinery is composed of ConB, ConC, ConD, ConE, ConG, CwlT, ConQ, and possibly other ICE*Bs1* proteins, and that ConB interacts with ConE, helping to recruit and/or maintain ConE at the membrane.


## IMPORTANCE

Conjugation is a major form of horizontal gene transfer and has played a profound role in bacterial evolution by moving genes, including those involved in antibiotic resistance,

metabolism, symbiosis, and infectious disease. During conjugation, DNA is transferred from cell to cell through the conjugation machinery, a type of secretion system. Relatively little is known about the conjugation machinery of Gram-positive bacteria. Here we analyzed five genes of the integrative and conjugative element ICE*Bs1* of *Bacillus subtilis*. Our research identifies four new components of the ICE*Bs1* conjugation machinery (ConB, ConC, ConD and ConG), and shows an interaction between ConB and ConE that is required for ConE to associate with the cell membrane.

## INTRODUCTION

Conjugation is a major form of horizontal gene transfer and plays a profound role in bacterial evolution and the acquisition of new traits (1-3). Conjugation can spread antibiotic resistance and disseminate genes involved in symbiosis, degradation of pollutants, metabolism, and pathogenesis. Conjugative elements encode specialized DNA translocation channels classified as Type IV secretion systems (T4SSs) (4-7). T4SSs are composed of many interacting proteins that span the envelope of the donor cell. In addition to transferring the conjugative DNA element, the conjugation machinery can also mobilize resident plasmids or other DNA elements that do not encode their own machinery.

There is a rich body of mechanistic and structural information on the T4SSs of Gram-negative bacteria (4, 7, 8). The Gram-negative T4SS is generally composed of 11 conserved mating-pair formation proteins (VirB1-VirB11, using the nomenclature of the *Agrobacterium tumefaciens* pTi plasmid) that form the DNA translocation channel along with a so-called "coupling protein" ATPase (VirD4) that delivers the relaxase-conjugative DNA nucleoprotein complex to the channel.

In comparison, much less is known about the "minimized" T4SSs of Gram-positive bacteria, which seem to be composed of a subset of the Gram-negative T4SS components (6-8). Conjugative elements from Gram positive organisms generally encode homologs to three T4SS proteins from Gram-negative bacteria: a VirD4-like coupling protein, a VirB1-like cell wall hydrolase, and a VirB4-like ATPase. In addition, elements from Gram positive bacteria encode proteins with similar structures and/or predicted membrane topologies and sizes to VirB3, VirB6, and VirB8. Many Gram-positive elements encode additional proteins that might also form part of the machinery.

The T4SSs of Gram-positive bacteria feature several significant differences from those found in Gram-negative bacteria, which is not surprising given the differences in the cell envelopes and sequences of the component proteins (6, 7). For example, Gram-positive elements do not encode homologs of any components that comprise the Gram-negative outer membrane "core complex," which plays crucial roles in T4SS assembly and gating. In addition, conjugative cell wall hydrolases are critical for conjugation in Gram-positive organisms (9-12), whereas they are generally dispensable for most Gram-negatives (13-15).

ICE*Bs1* is an integrative and conjugative element (ICE) found in the chromosome of *Bacillus subtilis* (reviewed in (16)). The genes needed for transfer of ICE*Bs1* are related to those from Tn*916* and ICE*St1* and other conjugative elements. ICE*Bs1* contains approximately two dozen open reading frames, many of which have been previously characterized for their roles in regulation, DNA processing, DNA replication, and conjugation (Fig. 1A) (9, 17-28). ICE*Bs1* normally resides stably integrated in *trnS-leu2*, the gene for a leucine tRNA, unless its major operon is derepressed (20). Derepression, and subsequent excision and mating, are induced upon DNA damage or when cells are crowded by potential recipients that do not have ICE*Bs1*. Upon

induction, ICE*Bs1* can transfer itself and mobilize resident plasmids, such as pBS42, that lack dedicated mobilization functions (26). Although plasmid mobilization requires ICE*Bs1*'s putative coupling protein ConQ, it does not require the ICE*Bs1* conjugative relaxase, ICE*Bs1* excision, or co-transfer with ICE*Bs1*. Thus, ICE*Bs1* is required to build the conjugation machinery allowing for mobilization to occur.

By analogy to other conjugation systems, the ICE*Bs1* conjugation machinery is likely composed of several interacting proteins. So far, the putative coupling protein ConQ (26), a VirB1-like cell wall hydrolase CwlT (9) and a VirB4-like ATPase ConE (27) are characterized components (Fig. 1A). Previously, we found that a fusion of ConE to a monomeric green fluorescent protein (GFP) localizes to the periphery of the cell membrane, with a large concentration found at the cell poles (27). One or more ICE*Bs1* proteins appear to be required for ConE to associate with the membrane, as ConE lacks predicted transmembrane segments and is found dispersed throughout the cytoplasm in cells lacking ICE*Bs1*.

We were interested in identifying other ICE*Bs1* genes needed for conjugation and determining which ICE*Bs1* proteins were needed for ConE to localize to the membrane. We constructed deletions in five ICE*Bs1* genes: *conB*, *conC*, *conD*, *conG* (previously *yddB*, *yddC*, *yddD*, *yddG*, respectively) and *yddF* (Fig. 1A). We then characterized the effects of the deletions on ICE*Bs1* transfer, plasmid mobilization, and localization of ConE-GFP. Together, our results are consistent with a model in which the ICE*Bs1* conjugation machinery is composed of putative transmembrane proteins ConB, ConC, ConD, ConG, along with the previously described ATPase ConE, cell wall hydrolase CwlT, and coupling protein ConQ. Furthermore, our results indicate that the peripheral membrane protein ConE is recruited to or kept at the membrane, at least in part, through direct interaction with ConB.

## MATERIALS AND METHODS

### Media and growth conditions

For *B. subtilis* and *Escherichia coli* strains, routine growth and strain constructions were done in LB medium. For all reported experiments with *B. subtilis*, cells were grown first in liquid LB at 37°C to an optical density (OD) 600nm of ~1.0. Cells were then diluted ~50-fold into LB or S7 defined minimal medium (29) with MOPS buffer at 50 mM rather than 100 mM, containing 1% glucose, 0.1% glutamate, and supplemented with auxotrophic requirements (40 μg/ml tryptophan; 40 μg/ml phenylalanine; 200 μg/ml threonine) as needed. Antibiotics were used at standard concentrations (30). For induction of ICE*Bs1*, 1 mM IPTG (isopropyl-β-D-thiogalactopyranoside) was added for 1-2 hours to overexpress *rapI* from Pspank(hy) in single copy on the chromosome at *amyE* (*amyE*::[(Pspank(hy)-*rapI*) *spc*]) as described previously (20).

### Strains, alleles, and plasmids

*E. coli* strains used for routine cloning were NEB 5α (New England Biolabs), AG115 (MC1061 F' *lacI*$^{q}$ *lacZ*::Tn*5*), and AG1111 (MC1061 F' *lacI*$^{q}$ *lacZ*M15 Tn*10*). *B. subtilis* strains and relevant genotypes are listed in Table 1; all are derivatives of JH642 containing the *trpC2* and *pheA1* mutations (31). *B. subtilis* strains were constructed by natural transformation (30). Strains cured of ICE*Bs1* (ICE*Bs1*$^{0}$), the spontaneous streptomycin resistance allele (*str-84*), the *amyE*::[Pspank(hy)-*rapI*) *spc*] allele, and Δ(*rapI phrI*)342::*kan* were described previously (20). The unmarked *conE(K476E)* allele, the complementation construct *thrC*::[(P*xis*-(*conD conE-lacZ*)) *mls*], and *lacA*::[P*xis*-(*conD conE-mgfpmut2*) *tet*] allele expressing *conD* and *conE-gfp* from the ectopic locus *lacA* were described previously (27). The *conQ848* deletion was described

previously (26). The *thrC325*::[(ICE*Bs1*-311 (Δ*attR*::*tet*)) *mls*] allele, containing ICE*Bs1* inserted at *thrC*, is incapable of excision due to deletion of the right attachment site *attR* as described previously (25). The truncation alleles ICE*Bs1*-319 (Fig. 1B) and ICE*Bs1*-320 (Fig. 1C) at *attB* have been described previously (25). pBS42 uses rolling circle replication, expresses chloramphenicol resistance in *B. subtilis*, lacks *mob/oriT*, and can be mobilized by ICE*Bs1* (26). All inserts in newly cloned plasmids were verified by sequencing.

***(i) Construction of unmarked in-frame gene deletions***

The basic strategy for constructing unmarked gene deletions was similar to that previously described for construction of *nicK306* (25). All gene deletions are unmarked, in-frame, and keep the upstream and downstream genes intact. *conB*Δ(9-350) deletes codons 9 through 350 of *conB*, resulting in the fusion of codons 1 through 8 to codons 351 through 357. *conC*Δ(5-81) deletes codons 5 through 81 of *conC*, resulting in the fusion of codons 1 through 4 to the last codon, 82. *conD*Δ(5-131) deletes codons 5 through 131 of *conD*, resulting in the fusion of codons 1 through 4 to codons 132 through 174. *yddF*Δ(5-103) deletes codons 5 through 103 of *yddF*, resulting in the fusion of codons 1 through 4 to codons 104 through 108. *conG*Δ(5-805) deletes codons 5 through 805 of *conG*, resulting in the fusion of codons 1 through 4 to codons 806 through 815. The splice-overlap-extension (SOE) PCR method (32) was used to generate DNA fragments containing the alleles. These fragments were cloned into the chloramphenicol resistance vector pEX44 (33) upstream of *lacZ*. The resulting plasmids were pMMB1257 for *conB*Δ(9-350), pMMB1251 for *conC*Δ(5-81), pMMB1253 for *conD*Δ(5-131), pMMB1252 for *yddF*Δ(5-103), and pMMB1254 for *conG*Δ(5-805). To replace the wild-type allele with the deleted gene, each plasmid was first integrated onto the chromosome of strain JMA168 by single crossover. The resulting strain was grown without selection for at least 20

generations, and loss of the plasmid was screened for by loss of both *lacZ* and chloramphenicol resistance. Detection of the desired unmarked deletion was confirmed by PCR.

***(ii) Construction of ICEBs1 single gene complementation alleles***

Complemented genes were cloned downstream of the IPTG-inducible promoter Pspank(hy). The *thrC*::[(Pspank(hy)-*conC*) *mls*] allele was constructed to express *conC*. *conC* was cloned into pCAL838, downstream of Pspank(hy), creating plasmid pMMB1338. pCAL838 allows for double crossover at the *thrC* locus in *B. subtilis*, and contains Pspank(hy), *lacI*, and *mls*. pMMB1338 was transformed into *B. subtilis* to create the *thrC*::[(Pspank(hy)-*conC*) *mls*] allele. A similar strategy was used to produce *thrC*::[(P*spank*(hy)-*conB*) *mls*] from plasmid pMMB1695, *thrC*::[(Pspank(hy)-*conD*) *mls*] from plasmid pMMB1339, *thrC*::[(Pspank(hy)-*yddF*) *mls*] from plasmid pMMB1340, and *thrC*::[(Pspank(hy)-*conG*) *mls*] from plasmid pMMB1341. For pMMB1695, an ATG start codon was used to replace the TTG native *conB* start codon, improving complementation (data not shown). For several genes tested, complementation was similar when genes were expressed from either Pspank(hy) or the ICE*Bs1* promoter Pxis, but was inferior when expressed from Pspank (data not shown).

***iii) Construction of truncated ICEBs1 complementation alleles***

Complementation of ConE-GFP localization in the Δ*conB* strain was tested using truncated ICE*Bs1* complementation constructs that cannot excise or transfer, similar to the strategy described previously (26). The truncated ICE*Bs1* derivative integrated at *thrC*, *thrC1755*::[ICE*Bs1* (Δ*conC*-*attR*::*cat*) *mls*], contains all of the ICE*Bs1* genes upstream of and including *conB* (Fig. 1D). The construct *thrC1756*::[ICE*Bs1* (Δ*conB*-*attR*::*cat*) *mls*] is essentially the same ICE*Bs1* insertion at *thrC*, but is missing *conB* (Fig. 1E). These alleles were constructed by transforming CAL1496, harboring *thrC325*::[(ICE*Bs1*-311 (Δ*attR*::*tet*)) *mls*], with SOE PCR

184 products that deleted the desired downstream region of ICE*Bs1*, replacing the tetracycline
185 resistance gene with a chloramphenicol resistance gene.
186 ***(iv) Conversion of Δ(rapI phrI)342::kan to Δ(rapI phrI)::cat***
187 The Δ(*rapI phrI*)342::*kan* allele (20) was altered to confer chloramphenicol resistance,
188 creating the Δ(*rapI phrI*)::*cat* allele. JMA168 was transformed with linearized pMMB1487,
189 selecting for resistance to chloramphenicol and screening for kanamycin sensitivity. pMMB1487
190 was constructed through isothermal assembly (34) so that it contains the *cat* gene flanked by
191 *yddK/rapI* and *yddM/yddN*.
192 ***(v) Construction of conE-gfp expressed from the conE locus in ICEBs1***
193 Strains MMB1547-1550 have the *conE* gene fused in frame to monomeric *gfpmut2*
194 (*mgfpmut2*) at its native locus in ICE*Bs1*. These strains were made by integrating pMMB1530
195 into the *B. subtilis* chromosome via a single crossover into *conE*. pMMB1530 contains the 3' end
196 of *conE* fused to DNA sequence encoding a 23 amino acid linker and *mgfpmut2*. The plasmid
197 was introduced into *B. subtilis* by transformation and selection for kanamycin resistance.
198 pMMB1530 was constructed by ligating the XhoI and SphI-cut vector from pMMB1445 with the
199 XhoI and SphI-cut fragment encoding the 23 amino acid linker and *mgfpmut2* from pLS31 (35).
200 pMMB1445 was constructed by inserting a PCR fragment containing the 3' end of *conE* into
201 pKL168 (36) digested with EcoRI and XhoI.
202 ***(vi) Construction of Pspank(hy) conB conC conD conE-gfp at thrC***
203 pMMB1702 was transformed into *B. subtilis* to create the *thrC*::[(Pspank(hy)-(*conB conC*
204 *conD conE-mgfpmut2*) *mls*] allele that expresses *conB, conC, conD and conE-mgfpmut2*.
205 pMMB1702 was constructed via isothermal assembly (34)of the PCR inserts (*conB conC conD*)

and (*conE-mgfpmut2*) into pCAL838 downstream of Pspank(hy). An ATG start codon was used to replace the native *conB* start codon TTG.

***(vii) Construction of bacterial two-hybrid protein fusions plasmids***

ICE*Bs1* genes were cloned in-frame into vectors carrying either the N-terminal (T25) or C-terminal (T18) portions of the *Bordetella pertussis cyaA* gene for adenylate cyclase as previously described (37). The plasmids encoding N- and C-terminal fusions of T18 to ConE were constructed by cloning into the BamHI/PstI sites of the vectors. pMMB1457 and pMMB1458 encode ampicillin resistance along with ConE-T18 and T18-ConE, respectively. Plasmids encoding N- and C-terminal fusions of T25 to ConB or ConD were constructed via isothermal assembly (34). pMMB1603, pMMB1604, pMMB1605, and pMMB1626 encode kanamycin resistance along with T25-ConD, ConB-T25, ConD-T25, and T25-ConB, respectively.

**Bacterial two hybrid interaction assays**

The bacterial two hybrid assays were performed similarly to prior reports (37). Two plasmids (one containing a T18-fusion and another containing a T25-fusion) were co-transformed into BTH101 [F-, *cya-99*, *araD139*, *gal15*, *galK16*, *rpsL1* (*Strlr*), *hsdR2*, *mcrA1*, *mcrB1*] *E. coli* competent cells. For negative controls, an empty vector was co-transformed with a T18/25-fusion protein or another empty vector. For qualitative analysis, the transformations were plated on MacConkey Base Agar supplemented with 0.1 % maltose, 0.1 mg/ml ampicillin, 0.05 mg/ml kanamycin, and 0.5 mM isopropyl β-D-1-thiogalactopyranoside (IPTG). The plates were incubated at 37°C overnight and then room temperature (~20°C) for an additional 24 hours for visual inspection of colony color. For quantitative assays, cells were grown shaking in LB

containing 0.1 mg/ml ampicillin, 0.05 mg/ml kanamycin and 0.5 mM IPTG at 30°C overnight for 14-16 hours. β-galactosidase activity was quantified as previously described (38). The reported results are averages of at least four independent experiments.

**Mating assays**

ICE*Bs1* mating was assayed as described previously (20). Briefly, donor cells contained a kanamycin resistance gene in ICE*Bs1*. Recipient cells (strain CAL419) lacked ICE*Bs1* (ICE*Bs1*$^0$) and were distinguishable from donors by being streptomycin resistant (*str-84*). Recipients were *comK* null to prevent acquisition of DNA via transformation. Cells were grown at least four generations to mid-exponential phase (OD600 to ~0.35) in minimal medium. ICE*Bs1* was induced in donors by addition of IPTG (1 mM) to induce expression of *rapI* from Pspank(hy). Donors and recipients were mixed 1:1 and filtered onto sterile cellulose nitrate membrane filters (0.2 μm pore size). Filters were placed in Petri dishes containing Spizizen's minimal salts (30) with 1.5% agar and incubated at 37°C for 3 hours. Cells were washed off the filter and the number of transconjugants was measured by determining the number of kanamycin- and streptomycin-resistant colony forming units (CFUs) after the mating. The number of donors was measured by determining the number of kanamycin-resistant CFUs after the mating. Percent mating is the (number of transconjugant CFUs per donor CFUs) x 100%. The reported results are averages of at least three independent experiments.

**Plasmid mobilization assays**

Mobilization of plasmid pBS42 by ICE*Bs1* was assayed essentially as described (26), similar to the mating assay described above. In addition to containing ICE*Bs1*, donor cells

252 contained the plasmid pBS42 and were grown with chloramphenicol (2.5 μg/mL) and kanamycin
253 (2.5 μg/mL) to maintain selection of the plasmid and ICE*Bs1*, respectively. The recipient strain
254 (CAL89) was ICE*Bs1*$^{0}$, streptomycin resistant (*str-84*) and *comK* null. Cells were grown at least
255 four generations to mid-exponential phase in LB medium before ICE*Bs1* was induced in donors
256 by addition of IPTG (1 mM) to induce expression of *rapI* from Pspank(hy). Mating was
257 performed on filters as described above. The number of pBS42 transconjugants was measured by
258 determining the number of chloramphenicol- and streptomycin-resistant CFUs. The number of
259 donors was measured by determining the number of chloramphenicol-resistant CFUs after the
260 mating. Plasmid mobilization efficiencies were calculated as the (number of pBS42
261 transconjugant CFUs per donor CFUs) x 100%. Transconjugants receiving ICE*Bs1* were also
262 monitored as described above for mating assays. The reported results are averages of at least
263 three independent experiments.
264
265 **Live-cell fluorescence microscopy**
266 Microscopy was performed as described (39). Cells were grown at least four generations
267 to mid-exponential phase in minimal medium. ICE*Bs1* was induced by addition of IPTG (1 mM)
268 to induce expression of *rapI* from Pspank(hy). Experiments using ConE-GFP were done with
269 strains that also contained a wild-type version of *conE* in ICE*Bs1*, except where noted. Live cells
270 were immobilized on pads of 1% agarose containing Spizizen's minimal salts and visualized at
271 room temperature. Some images were captured with a Nikon E800 microscope equipped with a
272 100x differential interference contrast objective, a Hamamatsu digital camera, and Chroma filter
273 set 41012 (for GFP). Improvision Openlabs 4.0 Software was used to process these images. The
274 remaining images were captured with a Nikon H550L microscope equipped with a 100x Plan

Fluor Phase Contrast Objective, a high resolution monochrome cooled CCD Andor digital camera, and Chroma filter set 96362 (for GFP). NIS Nikon Elements 4.0 Software was used to process these images. Each strain was examined in at least three independent experiments.

## RESULTS

### *conB, conC, conD,* and *conG* (but not *yddF*) are required for the conjugative transfer of ICE*Bs1*

We analyzed five ICE*Bs1* genes (*conB*, *conC*, *conD*, *yddF*, and *conG*; Fig. 1A) as each had characteristics that suggested it might encode a component of the ICE*Bs1* T4SS. ConB is a putative bitopic membrane protein homologous to conjugation proteins that are structurally similar, but not phylogenetically related, to VirB8 (40, 41). ConC is a putative integral membrane protein with two predicted transmembrane helices (8). Although ConC homologs are not widespread, some conjugative elements in Gram-positive organisms encode proteins of similar size and predicted topology. ConD contains two transmembrane helices and resembles VirB3 in terms of size and predicted topology (7, 8). *yddF* encodes a putative DNA-binding protein that is found mainly in crenarchaeal viruses (42, 43). It was analyzed here given its proximity to other predicted ICE*Bs1* T4SS genes (Fig. 1A) and the modular nature of ICEs where genes of shared function are often linked (44, 45). Lastly, *conG* encodes a conserved putative polytopic membrane protein analogous to VirB6 and was previously shown to be involved in ICE*Bs1* conjugation (7).

We constructed in-frame unmarked deletions of *conB, conC, conD, yddF,* and *conG* in ICE*Bs1* to determine whether these genes were required for mating. We compared mating efficiencies of ICE*Bs1* from donor strains containing the various deletions into recipient *B.*

298 *subtilis* cells lacking the conjugative element. The donor ICE*Bs1* contained a kanamycin
299 resistance marker that had been inserted to allow selection and monitoring of ICE*Bs1* acquisition
300 (20). We found that an ICE*Bs1*$^{+}$ donor strain transferred with an average mating frequency of
301 ~3% (percent transconjugant CFU per donor CFU; Fig. 2, row a), as seen previously (20).
302 Conjugation was undetectable from Δ*conB,* Δ*conC,* Δ*conD,* or Δ*conG* donor strains (Fig. 2, rows
303 b, d, f, i). Given our limit of detection, we estimate that mating is down at least 300,000-fold for
304 each. The Δ*yddF* donor strain mated similarly to wild type *B. subtilis* cells (Fig. 2, row h).
305 The defect in mating caused by each gene deletion was complemented at least partially
306 when the appropriate gene was reinserted at *thrC*, outside of ICE*Bs1* (Fig. 2). Only the *conG*
307 complementation construct restored mating to near wild type efficiency (Fig 2, row j). Mating
308 was restored at least 500-fold for *conB*, 1000-fold for *conC*, and 5000-fold for *conD* (Fig 2, rows
309 c, e, g). Attempts to improve complementation using alternative promoters to drive expression of
310 the complemented gene were not successful (See Materials and Methods). The mating frequency
311 of each strain was restored to near wild-type levels when a largely intact transfer-defective
312 ICE*Bs1* was inserted elsewhere on the chromosome (data not shown), indicating that the in-
313 frame deletions do not remove a *cis*-acting site required for conjugation. Partial complementation
314 is commonly observed for conjugative systems (27, 46) and could be due to unexpected effects
315 of the deletion on other ICE*Bs1* genes and/or insufficient expression of the complemented gene.
316 Based on prior work (27), we suspect that the conjugation proteins are not efficiently translated
317 and/or assembled into an active complex when expressed in *trans* to other ICE*Bs1* proteins.
318 Nevertheless, we conclude that *conB, conC, conD,* and *conG* are critical for the conjugative
319 transfer of ICE*Bs1*, while *yddF* appears to be dispensable under the conditions tested.
320

**ICE*Bs1* genes required for the mobilization of plasmid pBS42**

We predicted that *conB, conC, conD,* and *conG* are required for the conjugative transfer of ICE*Bs1* because they encode critical components of the ICE*Bs1* DNA translocation channel. Alternatively, these genes could be important for other aspects of ICE*Bs1* biology. For example, they could be critical for excision, replication or integration of ICE*Bs1*. To distinguish these possibilities, we tested whether these genes were required for plasmid mobilization. Mobilization would require the ICE*Bs1* conjugation machinery, but would not require genes involved in ICE*Bs1* DNA processing events (26).

We found that *conB, conC, conD, conE,* and *conG* were required for the ICE*Bs1*-mediated mobilization of plasmid pBS42 (Fig. 3). The same mating procedure was used as above, except that the ICE*Bs1*$^{+}$ donor strains also contained pBS42, a plasmid that confers chloramphenicol resistance allowing measurement of its acquisition. As seen previously (26), a wild type donor strain (ICE*Bs1*$^{+}$) transferred pBS42 with an average mobilization frequency of ~2% (Fig. 3, row a). Mobilization of pBS42 was not detectable from donor strains containing deletions in *conB, conC, conD,* or *conG* or a donor strain containing a missense mutation (K476E) in the ATP-binding motif (Walker A box) of ConE (Fig. 3, rows b, d, f, h, l). We estimate that plasmid mobilization is down at least 10,000-fold for each of these mutants. The Δ*yddF* donor strain mobilized pBS42 at a frequency of 0.07%, ~30-fold lower than wild type (Fig. 3, row j), indicating that *yddF* contributes, at least modestly, to efficient pBS42 transfer. As observed for the mating assays, mobilization was partially complemented when the genes were expressed *in trans* (Fig. 3, rows c, e, g, i, k, m). Taken together with their predicted membrane locations and sequence conservation, these results indicate that ConB, ConC, ConD, and ConG are likely components of the ICE*Bs1* DNA translocation channel since they are required for both

conjugation of ICE*Bs1* and plasmid mobilization. YddF does not seem to be a critical component of the channel since it is not conserved in other conjugative elements, was not required for ICE*Bs1* transfer, and made only a minor contribution to plasmid mobilization.

**_conB,_ and to some extent _conD,_ are required for ConE-GFP localization at the cell membrane**

ConE-GFP localizes to the membrane, predominantly at the cell poles, when ICE*Bs1* gene expression is induced (27). In contrast, ConE-GFP mislocalizes to the cytoplasm in cells lacking ICE*Bs1*. These results indicate that at least one ICE*Bs1* gene product may recruit and/or retain ConE at the membrane. The four ICE*Bs1* proteins shown above to be required for both mating and mobilization (ConB, ConC, ConD and ConG) all contain at least one predicted transmembrane helix (Fig. 1A). To test whether any of these proteins might be required for ConE membrane localization, we examined the subcellular localization of ConE-GFP in strains containing large deletions of ICE*Bs1*. We used a construct in which *conE-gfp* is expressed from the ICE*Bs1* promoter Pxis, together with the upstream gene *conD*, at a heterologous locus (*lacA*) as previously described (27). *conD* was included upstream of *conE-gfp* as ConE-GFP is not detectable in cells in the absence of *conD* in this context (data not shown). We observed ConE-GFP at the membrane preferentially at the cell poles in cells containing an intact ICE*Bs1* (Fig. 4a), as seen previously (27). Furthermore, we found that ConE-GFP localized properly in a strain that contained a large deletion starting midway through *conG* through to *yddM* (Fig. 1B; Fig. 4b). Thus, ConE localization does not require the C-terminus of ConG, nor the seven ICE*Bs1* proteins encoded downstream (CwlT, YddI, YddJ, YddK, RapI, PhrI, and YddM). In contrast, we found that ConE-GFP mislocalized to the cytoplasm in a strain containing a larger deletion spanning

367 from *conB* to *yddM* (Fig. 1C; Fig. 4c). Previous experiments demonstrated that ConE-GFP
368 expressed from *lacA* does not require wild type *conE* in ICE*Bs1* for proper localization (27).
369 Therefore, we conclude that ConB, ConC, ConD, YddF, and/or a part of ConG are required for
370 localization of ConE-GFP.

371 To narrow down the requirements, we visualized ConE-GFP in strains containing single
372 in-frame unmarked gene deletions. We found that ConE-GFP was dispersed throughout the
373 cytoplasm in Δ*conB* cells (Fig. 4d). Localization was restored in Δ*conB* cells with addition of an
374 ICE*Bs1* at an ectopic locus that contained the genes up to and including *conB* (Fig. 1D; data not
375 shown), but localization was not restored with addition of an ICE*Bs1* that contained the genes up
376 to but not including *conB* (Fig. 1E; data not shown), indicating that the defect in localization of
377 ConE-GFP in the absence of *conB* was not due to polarity on downstream genes. ConE-GFP
378 targeted normally to the membrane in strains containing single gene deletions of *conC*, *yddF,* or
379 *conG* (Fig. 4e, g, h). These results indicate that proper localization of ConE requires *conB*, but
380 not *conC* or any of the genes from *conE-yddM*.

381 Since expression of ConE-GFP at *lacA* required the presence of the upstream gene c*onD*,
382 we were unable to use this construct to test whether *conD* is required for ConE-GFP localization.
383 Therefore, we fused *gfp* downstream of *conE* in its native position in ICE*Bs1*. To confirm that
384 this new construct recapitulates ConE-GFP localization, we first examined ConE-GFP in this
385 strain and in strains deleted for *conB* or *conC*. As expected, ConE-GFP localized properly in the
386 parental and Δ*conC* strains, but mislocalized in Δ*conB* cells (data not shown). We next
387 examined ConE-GFP in Δ*conD* cells. We observed a partial defect in localization in the Δ*conD*
388 strain (Fig. 4f). ConE-GFP localized to the membrane preferentially at the cell poles in most
389 cells, however, a large proportion of ConE-GFP was also found dispersed throughout the

cytoplasm. Localization of ConE-GFP in a Δ*conD* strain was restored when *conD* was added back *in trans* (data not shown).

We also tested ConE-GFP localization in a Δ*conQ* strain, as ConQ is the only ICE*Bs1* transmembrane protein that had not been tested (Fig. 1A). We found that ConE-GFP localized normally in the absence of the presumed coupling protein ConQ (Fig. 4i). We conclude that ConB, and to some extent ConD, are required for recruiting and/or maintaining ConE at the membrane. Furthermore, our results show that *conQ*, *conC*, and the ten genes from *conE* to *yddM* (Fig. 1A) are not required for ConE-localization. Previously, we showed that *xis*, which encodes the excisionase, was also not required for ConE localization (27).

To determine whether ConB and ConD are sufficient for ConE's localization, we placed *conB*, *conC*, *conD*, and *conE-gfp* at an ectopic locus under control of an inducible promoter. The genes were cloned in tandem, as arranged in ICE*Bs1*, and placed on the chromosome in a strain lacking ICE*Bs1*. We found that ConE-GFP largely mislocalized to the cytoplasm in these cells (Fig. 4j). Most cells contained several foci or clusters of GFP fluorescence, oftentimes localized near the membrane and cell poles. We hypothesize that the foci of ConE-GFP are formed due to formation of subsets of the conjugation machinery proteins. When ConE-GFP is expressed in the presence of ConD alone, it mislocalizes to the cytoplasm uniformly and does not form small foci (27), indicating that ConB and/or ConC might be involved in formation of the clusters. Furthermore, the result indicates that while ConB and ConD are required for the localization of ConE to the membrane, they may not be sufficient. Ten ICE*Bs1* proteins encoded upstream of *conB* (excluding ConQ and Xis) have not been tested and may also play a role. The best candidates include uncharacterized ICE*Bs1* proteins such as YdzL, YdcO, YdcS, YdcT, and YddA, although none of these are predicted membrane proteins. Alternatively, ConB and ConD

may be sufficient, but they are not produced in the correct stoichiometry and/or targeted correctly when expressed from an ectopic locus. This second interpretation is consistent with our complementation data (Fig. 2 and 3) that indicate mating proteins do not function optimally when expressed *in trans*.

**ConE and ConB interact in a bacterial two hybrid assay**

Our results indicate that ConB, and to some extent ConD, are required for localization of ConE to the membrane. To test whether ConE directly interacts with either protein, we used a bacterial two hybrid assay that is based on the interaction between the T18 and T25 domains of the *Bordetella pertussis* enzyme adenylate cyclase (37). If the two domains are fused to interacting proteins, cAMP is produced, resulting in increased expression of a *lacZ* reporter gene. Because the enzyme is cytoplasmic and does not rely on interactions with DNA, it has been useful for detecting interactions between membrane proteins, including components of T4SSs (40, 47-49). As we were uncertain as to whether attachment of T18 or T25 at the N- or C-terminus of a protein would interfere with interaction or targeting, we made both types of fusions. Therefore, we constructed plasmids that encode ConE-T18 and T18-ConE, along with ConB-T25, T25-ConB, ConD-T25, and T25-ConD.

We co-transformed plasmids encoding T18 and T25 fusion proteins and assayed their interactions by measuring β-galactosidase activity. Negative controls were cells co-transformed with one plasmid encoding a fusion protein (e.g., ConE-T18) and one empty vector. Of the four predator-prey ConE-ConB combinations tested, three showed statistically higher levels of β-galactosidase activity (P-value $<0.05$) than the corresponding negative controls (~80 Miller units; Fig. 5). No statistically significant interactions were detected between ConE and ConD (Fig. 5).

These data indicate that ConE and ConB may directly interact *in vivo*.

## DISCUSSION

We found that *conB, conC, conD,* and *conG* are required for conjugative transfer of ICE*Bs1* and mobilization of pBS42. Homologs of these genes are found in other conjugative elements in Gram-positive bacteria and encode putative integral membrane proteins. We propose a model in which the ICE*Bs1* T4SS is composed of ConB, ConC, ConD, ConG, along with the previously described ConE ATPase, presumed coupling protein ConQ, and cell wall hydrolase CwlT (Fig. 6). Similar models have recently been proposed for the conjugative plasmid pCW3 of *Clostridium perfringens* (10, 40, 46, 48, 50, 51), the broad-host range conjugative plasmid pIP501(12, 41, 52), and pCF10 of *Enterococcus faecalis* (11, 53, 54), indicating that a general consensus is building as to the composition of the Gram-positive T4SS.

ConG and ConB may form a major portion of the ICE*Bs1* DNA translocation channel within the membrane. ConG is large (815 amino acids long) and the N-terminal half is predicted to have seven transmembrane segments (Fig. 6). ConG likely forms higher-order oligomers as seen for the Gram-positive homolog TcpH (47). ConB is shorter (354 amino acids long) and bitopic with two tandem NTF2-like domains outside the cell membrane (40, 41). The extracytoplasmic domains of homologs of ConB crystallize as trimers. Given ConE's cytoplasmic location, we propose that ConE directly interacts with the short intracellular N-terminal tail of ConB (Fig. 6).

Recently, a low resolution 3 megadalton structure of a Gram-negative T4SS was determined using electron microscopy (55). Biochemical analysis of the complex indicates that most of the inner membrane components form very large oligomers within the T4SS. Notably,

VirB3 and VirB8 appear to be 12-mers, VirB6 a 24-mer, and VirB4 is associated with the T4SS as two separate hexameric rings on the cytoplasmic face of the complex. It will be interesting to determine whether the Gram-positive counterparts form a complex with similarly large oligomeric proportions.

In our model, the peripheral membrane protein ConE likely associates with the ICE*Bs1* T4SS through direct interaction with ConB. This interaction was supported by bacterial two hybrid data (Fig. 5) and the observation that ConE-GFP's localization to the membrane depended upon *conB* (Fig. 4d). Two lines of evidence indicate a potential interaction between ConE and ConD. First, a large proportion of ConE-GFP mislocalizes to the cytoplasm in Δ*conD* cells (Fig. 4f). Second, *conD* and *conE* (and their homologs) are linked genetically. *conD* is encoded directly upstream of and translationally overlaps with *conE* in ICE*Bs1*. In many organisms, the *virB3*-like gene is directly fused to the *virB4* gene (8). Fusion of the T18 or T25 domains to ConE and ConD may have prevented their interaction in bacterial two hybrid assays. More studies are necessary to address whether ConE and ConD indeed directly interact.

VirB4 proteins like ConE localize to the membrane, but the precise localization patterns are specific to each conjugative element. For example, TcpF of pCW3 localizes to the cell poles (47) and VirB4 of the *B. subtilis* plasmid pLS20 localizes at a single pole and at several sites along the membrane (56). In contrast, both VirB4 of *A. tumefaciens* and TrhC of the *E. coli* R27 conjugative plasmid localize to several foci along the periphery of the cell membrane (57, 58). While ConE requires only two of the seven other known ICE*Bs1* T4SS proteins for its localization, TrhC requires 12 different R27 T4SS proteins (58). All 12 proteins likely do not interact directly with TrhC; rather, this group of proteins may form an ordered network of

interacting proteins whereby disruption of initializing components could result in incomplete assembly and mislocalization of TrhC.

The ICE*Bs1* protein YddF was not required for conjugation and is not conserved in other conjugative elements. While the function of YddF is still unclear, our results indicate that this putative DNA-binding protein may, in part, facilitate plasmid mobilization (Fig. 3). This effect could be indirect, such as *yddF* increasing pBS42 copy number. While YddF was dispensable for transfer of ICE*Bs1* under our conditions, YddF could be required when mating into other types of bacteria or under different conditions. Nevertheless, YddF is not a critical component of the ICE*Bs1* T4SS.

Together, our results provide a first model for the T4SS of ICE*Bs1* (Fig. 6). Future experiments will be required to verify the predicted topologies of the protein components and determine their protein-protein interactions and functions.

**ACKNOWLEDGEMENTS**

We would like to thank Suffolk undergraduate students Naira Aleksanyan, Georgeanna Morton, April Culannay, Stefanie Baril, Omar Pinkhasov and former class members of CHEM L333 for their contributions to this project. We would like to thank Edith Enyedy for technical assistance and the chemistry and biology faculty at Suffolk University for their support. We thank Jacob Thomas at the Georgia Institute of Technology and Briana Burton of Harvard University for helpful advice, Kenneth Briley and David Dubnau at the Public Health Research Institute for useful vectors, and Laurel Wright and Chris Johnson of the Massachusetts Institute of Technology for helpful comments on the manuscript. This work was supported, in part, by the National Science Foundation Research at Undergraduate Institution program (NSF-RUI Grant

1157878 to MBB), the National Institute of General Medical Sciences of the National Institutes of Health (R01GM50895 to ADG), and a Suffolk University Summer Stipend Award (MBB).

## REFERENCES

1. **Wiedenbeck J, Cohan FM.** 2011. Origins of bacterial diversity through horizontal genetic transfer and adaptation to new ecological niches. FEMS Microbiol Rev **35:**957-976.
2. **Gogarten JP, Townsend JP.** 2005. Horizontal gene transfer, genome innovation and evolution. Nat Rev Microbiol **3:**679-687.
3. **Frost LS, Leplae R, Summers AO, Toussaint A.** 2005. Mobile genetic elements: the agents of open source evolution. Nat Rev Microbiol **3:**722-732.
4. **Waksman G, Fronzes R.** 2010. Molecular architecture of bacterial type IV secretion systems. Trends Biochem Sci **35:**691-698.
5. **Smillie C, Garcillan-Barcia MP, Francia MV, Rocha EP, de la Cruz F.** 2010. Mobility of plasmids. Microbiol Mol Biol Rev **74:**434-452.
6. **Goessweiner-Mohr N, Arends K, Keller W, Grohmann E.** 2013. Conjugative type IV secretion systems in Gram-positive bacteria. Plasmid **70:**289-302.
7. **Bhatty M, Laverde Gomez JA, Christie PJ.** 2013. The expanding bacterial type IV secretion lexicon. Res Microbiol **164:**620-639.
8. **Alvarez-Martinez CE, Christie PJ.** 2009. Biological diversity of prokaryotic type IV secretion systems. Microbiol Mol Biol Rev **73:**775-808.
9. **DeWitt T, Grossman AD.** 2014. The bifunctional cell wall hydrolase CwlT is needed for conjugation of the integrative and conjugative element ICE*Bs1* in *Bacillus subtilis* and *B.*

*anthracis*. J Bacteriol **196:**1588-1596.

10. **Bantwal R, Bannam TL, Porter CJ, Quinsey NS, Lyras D, Adams V, Rood JI.** 2012. The peptidoglycan hydrolase TcpG is required for efficient conjugative transfer of pCW3 in *Clostridium perfringens*. Plasmid **67:**139-147.

11. **Laverde Gomez JA, Bhatty M, Christie PJ.** 2013. PrgK, a multidomain peptidoglycan hydrolase, is essential for conjugative transfer of the pheromone-responsive plasmid pCF10. J Bacteriol **196:**527-539.

12. **Arends K, Celik EK, Probst I, Goessweiner-Mohr N, Fercher C, Grumet L, Soellue C, Abajy MY, Sakinc T, Broszat M, Schiwon K, Koraimann G, Keller W, Grohmann E.** 2013. TraG encoded by the pIP501 type IV secretion system is a two-domain peptidoglycan-degrading enzyme essential for conjugative transfer. J Bacteriol **195:**4436-4444.

13. **Berger BR, Christie PJ.** 1994. Genetic complementation analysis of the *Agrobacterium tumefaciens virB* operon: *virB2* through *virB11* are essential virulence genes. J Bacteriol **176:**3646-3660.

14. **Bayer M, Eferl R, Zellnig G, Teferle K, Dijkstra A, Koraimann G, Hogenauer G.** 1995. Gene 19 of plasmid R1 is required for both efficient conjugative DNA transfer and bacteriophage R17 infection. J Bacteriol **177:**4279-4288.

15. **Winans SC, Walker GC.** 1985. Conjugal transfer system of the IncN plasmid pKM101. J Bacteriol **161:**402-410.

16. **Berkmen MB, Laurer SJ, Giarusso BK, Romero R.** 2013. The Integrative and Conjugative Element ICE*Bs1* of *Bacillus subtilis*. *In* Roberts AP, Mullany P (ed), Bacterial Integrative Mobile Genetic Elements. Landes Biosciences, Austin.

17. **Babic A, Berkmen MB, Lee CA, Grossman AD.** 2011. Efficient gene transfer in bacterial cell chains. mBio **2**(2)**:** e00027-11. doi:10.1128/mBio.00027-11.

18. **Thomas J, Lee CA, Grossman AD.** 2013. A conserved helicase processivity factor is needed for conjugation and replication of an integrative and conjugative element. PLoS Genet **9:**e1003198. doi:10.1371/journal.pgen.1003198.

19. **Auchtung JM, Lee CA, Garrison KL, Grossman AD.** 2007. Identification and characterization of the immunity repressor (ImmR) that controls the mobile genetic element ICE*Bs1* of *Bacillus subtilis*. Mol Microbiol **64:**1515-1528.

20. **Auchtung JM, Lee CA, Monson RE, Lehman AP, Grossman AD.** 2005. Regulation of a *Bacillus subtilis* mobile genetic element by intercellular signaling and the global DNA damage response. Proc Natl Acad Sci U S A **102:**12554-12559.

21. **Bose B, Auchtung JM, Lee CA, Grossman AD.** 2008. A conserved anti-repressor controls horizontal gene transfer by proteolysis. Mol Microbiol **70:**570-582.

22. **Bose B, Grossman AD.** 2011. Regulation of horizontal gene transfer in *Bacillus subtilis* by activation of a conserved site-specific protease. J Bacteriol **193:**22-29.

23. **Lee CA, Auchtung JM, Monson RE, Grossman AD.** 2007. Identification and characterization of *int* (integrase), *xis* (excisionase) and chromosomal attachment sites of the integrative and conjugative element ICE*Bs1* of *Bacillus subtilis*. Mol Microbiol **66:**1356-1369.

24. **Lee CA, Babic A, Grossman AD.** 2010. Autonomous plasmid-like replication of a conjugative transposon. Mol Microbiol **75:**268-279.

25. **Lee CA, Grossman AD.** 2007. Identification of the origin of transfer (*oriT*) and DNA relaxase required for conjugation of the integrative and conjugative element ICE*Bs1* of

*Bacillus subtilis*. J Bacteriol **189:**7254-7261.

26. **Lee CA, Thomas J, Grossman AD.** 2012. The *Bacillus subtilis* conjugative transposon ICE*Bs1* mobilizes plasmids lacking dedicated mobilization functions. J Bacteriol **194:**3165-3172.

27. **Berkmen MB, Lee CA, Loveday EK, Grossman AD.** 2010. Polar positioning of a conjugation protein from the integrative and conjugative element ICE*Bs1* of *Bacillus subtilis*. J Bacteriol **192:**38-45.

28. **Johnson CM, Grossman AD.** 2014. Identification of host genes that affect acquisition of an integrative and conjugative element in *Bacillus subtilis*. Mol Microbiol **93:**1284-1301.

29. **Vasantha N, Freese E.** 1980. Enzyme changes during *Bacillus subtilis* sporulation caused by deprivation of guanine nucleotides. J Bacteriol **144:**1119-1125.

30. **Harwood CR, Cutting SM.** 1990. Molecular Biological Methods for *Bacillus*. John Wiley & Sons, Chichester.

31. **Perego M, Spiegelman GB, Hoch JA.** 1988. Structure of the gene for the transition state regulator, *abrB*: regulator synthesis is controlled by the *spo0A* sporulation gene in *Bacillus subtilis*. Mol Microbiol **2:**689-699.

32. **Horton RM, Hunt HD, Ho SN, Pullen JK, Pease LR.** 1989. Engineering hybrid genes without the use of restriction enzymes: gene splicing by overlap extension. Gene **77:**61-68.

33. **Comella N, Grossman AD.** 2005. Conservation of genes and processes controlled by the quorum response in bacteria: characterization of genes controlled by the quorum-sensing transcription factor ComA in *Bacillus subtilis*. Mol Microbiol **57:**1159-1174.

34. **Gibson DG, Young L, Chuang RY, Venter JC, Hutchison CA, 3rd, Smith HO.** 2009.

Enzymatic assembly of DNA molecules up to several hundred kilobases. Nat Methods **6:**343-345.

35. **Simmons LA, Davies BW, Grossman AD, Walker GC.** 2008. Beta clamp directs localization of mismatch repair in *Bacillus subtilis*. Mol Cell **29:**291-301.

36. **Lemon KP, Grossman AD.** 1998. Localization of bacterial DNA polymerase: evidence for a factory model of replication. Science **282:**1516-1519.

37. **Karimova G, Ullmann A, Ladant D.** 2000. A bacterial two-hybrid system that exploits a cAMP signaling cascade in *Escherichia coli*. Methods Enzymol **328:**59-73.

38. **Miller JH.** 1972. Experiments in Molecular Genetics. Cold Spring Harbor Laboratory Press, Cold Spring Harbor, NY.

39. **Berkmen MB, Grossman AD.** 2006. Spatial and temporal organization of the *Bacillus subtilis* replication cycle. Mol Microbiol **62:**57-71.

40. **Porter CJ, Bantwal R, Bannam TL, Rosado CJ, Pearce MC, Adams V, Lyras D, Whisstock JC, Rood JI.** 2012. The conjugation protein TcpC from *Clostridium perfringens* is structurally related to the type IV secretion system protein VirB8 from Gram-negative bacteria. Mol Microbiol **83:**275-288.

41. **Goessweiner-Mohr N, Grumet L, Arends K, Pavkov-Keller T, Gruber CC, Gruber K, Birner-Gruenberger R, Kropec-Huebner A, Huebner J, Grohmann E, Keller W.** 2013. The 2.5 A structure of the enterococcus conjugation protein TraM resembles VirB8 type IV secretion proteins. J Biol Chem **288:**2018-2028.

42. **Keller J, Leulliot N, Cambillau C, Campanacci V, Porciero S, Prangishvilli D, Forterre P, Cortez D, Quevillon-Cheruel S, van Tilbeurgh H.** 2007. Crystal structure of AFV3-109, a highly conserved protein from crenarchaeal viruses. Virol J **4:**12.

43. **Larson ET, Eilers BJ, Reiter D, Ortmann AC, Young MJ, Lawrence CM.** 2007. A new DNA binding protein highly conserved in diverse crenarchaeal viruses. Virology **363:**387-396.

44. **Wozniak RA, Waldor MK.** 2010. Integrative and conjugative elements: mosaic mobile genetic elements enabling dynamic lateral gene flow. Nat Rev Microbiol **8:**552-563.

45. **Burrus V, Waldor MK.** 2004. Shaping bacterial genomes with integrative and conjugative elements. Res Microbiol **155:**376-386.

46. **Bannam TL, Teng WL, Bulach D, Lyras D, Rood JI.** 2006. Functional identification of conjugation and replication regions of the tetracycline resistance plasmid pCW3 from *Clostridium perfringens*. J Bacteriol **188:**4942-4951.

47. **Teng WL, Bannam TL, Parsons JA, Rood JI.** 2008. Functional characterization and localization of the TcpH conjugation protein from *Clostridium perfringens*. J Bacteriol **190:**5075-5086.

48. **Steen JA, Bannam TL, Teng WL, Devenish RJ, Rood JI.** 2009. The putative coupling protein TcpA interacts with other pCW3-encoded proteins to form an essential part of the conjugation complex. J Bacteriol **191:**2926-2933.

49. **de Paz HD, Larrea D, Zunzunegui S, Dehio C, de la Cruz F, Llosa M.** 2010. Functional dissection of the conjugative coupling protein TrwB. J Bacteriol **192:**2655-2669.

50. **Wisniewski JA, Teng WL, Bannam TL, Rood JI.** 2014. Two novel membrane proteins TcpD and TcpE are essential for conjugative transfer of pCW3 in *Clostridium perfringens*. J Bacteriol **197**:774-781.

51. **Parsons JA, Bannam TL, Devenish RJ, Rood JI.** 2007. TcpA, an FtsK/SpoIIIE

642 homolog, is essential for transfer of the conjugative plasmid pCW3 in *Clostridium*
643 *perfringens*. J Bacteriol **189:**7782-7790.
644 52. **Abajy MY, Kopec J, Schiwon K, Burzynski M, Doring M, Bohn C, Grohmann E.**
645 2007. A type IV-secretion-like system is required for conjugative DNA transport of
646 broad-host-range plasmid pIP501 in gram-positive bacteria. J Bacteriol **189:**2487-2496.
647 53. **Li F, Alvarez-Martinez C, Chen Y, Choi KJ, Yeo HJ, Christie PJ.** 2012.
648 *Enterococcus faecalis* PrgJ, a VirB4-like ATPase, mediates pCF10 conjugative transfer
649 through substrate binding. J Bacteriol **194:**4041-4051.
650 54. **Chen Y, Zhang X, Manias D, Yeo HJ, Dunny GM, Christie PJ.** 2008. *Enterococcus*
651 *faecalis* PcfC, a spatially localized substrate receptor for type IV secretion of the pCF10
652 transfer intermediate. J Bacteriol **190:**3632-3645.
653 55. **Low HH, Gubellini F, Rivera-Calzada A, Braun N, Connery S, Dujeancourt A, Lu**
654 **F, Redzej A, Fronzes R, Orlova EV, Waksman G.** 2014. Structure of a type IV
655 secretion system. Nature **508:**550-553.
656 56. **Bauer T, Rosch T, Itaya M, Graumann PL.** 2011. Localization pattern of conjugation
657 machinery in a Gram-positive bacterium. J Bacteriol **193:**6244-6256.
658 57. **Aguilar J, Cameron TA, Zupan J, Zambryski P.** 2011. Membrane and core
659 periplasmic *Agrobacterium tumefaciens* virulence Type IV secretion system components
660 localize to multiple sites around the bacterial perimeter during lateral attachment to plant
661 cells. mBio **2**(6)**:**e00218-00211. doi:10.1128/mBio.00218-11.
662 58. **Gilmour MW, Taylor DE.** 2004. A subassembly of R27-encoded transfer proteins is
663 dependent on TrhC nucleoside triphosphate-binding motifs for function but not
664 formation. J Bacteriol **186:**1606-1613.

665 59. **Käll L, Krogh A, Sonnhammer EL.** 2005. An HMM posterior decoder for sequence
666 feature prediction that includes homology information. Bioinformatics **21** Suppl 1**:**i251-
667 257.
668 60. **Zhou M, Boekhorst J, Francke C, Siezen RJ.** 2008. LocateP: genome-scale
669 subcellular-location predictor for bacterial proteins. BMC Bioinformatics **9:**173.
670
671

672 **FIGURE LEGENDS**

673 **FIG 1.** Genetic structure of ICE*Bs1* and its derivatives. (A). Schematic of ICE*Bs1* integrated at
674 the normal attachment site, *attB*. Each ORF (arrowed box oriented in the direction of its
675 transcription) and *attL* and *attR* (black boxes) are indicated. Previously characterized genes that
676 encode ICE*Bs1* conjugation machinery are shaded in black. Genes shown here to be required for
677 conjugation are shaded in grey. The number of predicted transmembrane helices (TMH) for each
678 protein is indicated below each gene. Predictions were obtained from Polyphobius, a HMM
679 topology prediction program that uses homology information (59), guided by the bacterial
680 subcellular location and secretion prediction program LocateP (60). Other topology programs
681 yield similar but not identical predictions. Genes that encode proteins with homology or
682 predicted structural similarity or membrane topology to *A. tumefaciens* pTi VirB/D T4SS
683 components are designated below. An antibiotic resistance marker (*kan* or *cam*) is inserted in
684 *rapI-phrI* in most strains, but is not shown. (B-E). Diagram of truncated ICE*Bs1* derivatives that
685 were used to analyze ConE-GFP localization. (B-C) Derivatives of ICE*Bs1*, ICE*Bs1*-319
686 (Δ*conG-yddM*) and ICE*Bs1*-320 (Δ*conB-yddM*), at *attB* have the genes indicated by the
687 horizontal line from *attL* to the middle of *conG* (B) or *conB* (C). (D-E) Truncated ICE*Bs1*
688 derivatives integrated at *thrC*, *thrC1755*::ICE*Bs1* (Δ*conC-attR*) and *thrC*, *thrC1756*::ICE*Bs1*
689 (Δ*conB-attR*), have the genes indicated by the horizontal line from *attL* and up to and including
690 *conB* (D) or *yddA* (E).

691

692 **FIG 2.** *conB*, *conC*, *conD*, and *conG* are required for mating of ICE*Bs1*. Cells were grown in
693 minimal glucose medium. The indicated donor cells [all containing Δ(*rapIphrI*)*342::kan* in
694 ICE*Bs1* and *amyE*::(Pspank(hy)-*rapI*)] were mated with ICE*Bs1*$^{0}$ *comK*::*cat str-84* recipient cells
695 (CAL419). Percent mating is the (number of transconjugant CFUs per donor CFU) x 100%. Data

696 are averages from at least three experiments. Error bars indicate the standard deviation. An
697 asterisk (*) indicates no detectable transconjugants (<1 x$10^{-5}$%). Donor strains were: JMA168
698 (a), MMB1275 (b), MMB1735 (c), MMB1271 (d), MMB1390 (e), MMB1274 (f), MMB1397
699 (g), MMB1273 (h), MMB1283 (i), and MMB1393 (j).
700
701 **FIG 3**. *conB*, *conC*, *conD*, *conE*, and *conG* are required for ICE*Bs1*-mediated mobilization of
702 pBS42. Cells were grown in LB. The indicated donor cells [all containing pBS42 (*cam*),
703 Δ(*rapIphrI)342::kan* in ICE*Bs1* and *amyE*::(Pspank(hy)-*rapI*)] were mated with ICE*Bs1*$^0$
704 *comK*::*spc str-84* recipient cells (CAL89). Percent mobilization is the (number of plasmid-
705 bearing transconjugant CFUs per donor CFU) x 100%. Data are averages from at least three
706 experiments. Error bars indicate the standard deviation. An asterisk (*) indicates no detectable
707 plasmid-bearing transconjugants (<4 x$10^{-4}$%). Donor strains were: MMB1473 (a), MMB1474
708 (b), MMB1760 (c), MMB1476 (d), MMB1477 (e), MMB1478 (f), MMB1479 (g), MMB1480
709 (h), MMB1481(i), MMB1482 (j), MMB1483 (k), MMB1484 (l), and MMB1485 (m).
710
711 **FIG 4**. *conB,* and to some extent *conD,* are required for localization of ConE-GFP at the cell
712 membrane. Cells were grown in minimal glucose medium. The indicated genotypes (see also
713 Table 1) were analyzed by live fluorescence microscopy. ConE-GFP fluorescence is shown in
714 green. (a) MMB968; (b) MMB1425; (c) MMB1426; (d) MMB1297; (e) MMB1293; (f)
715 MMB1549; (g) MMB1343; (h) MMB1299; (i) MMB1247; (j) MMB1715. All cells were
716 induced with 1 mM IPTG for one hour, except panel h for two hours. ConE-GFP targeted
717 normally in a strain deleted for *conG*, but the targeting required IPTG induction for two hours
718 instead of one hour. We observed no differences in mating, mobilization, and ConE-GFP

719 localization for one versus two hour induction for wild-type strains.

720

721 **FIG 5.** ConE interacts with ConB *in vivo* in bacterial two-hybrid assays. Quantitative β-
722 galactosidase assays were performed on strains with plasmids expressing T18 and T25 fusion
723 proteins. Strains contained plasmids expressing either T18-ConE (T18-E) or ConE-T18(E-T18).
724 Strains also contained a plasmid expressing ConB-T25(B-T25), T25-ConB(T25-B), ConD-
725 T25(D-T25), or T25-ConD (T25-D). The average β-galactosidase activity and standard error of
726 the mean are reported. The average β-galactosidase activity of the negative controls, expressing
727 one fusion protein and one empty vector, is represented by the dotted line. A statistically
728 significant P-value (<0.05), as determined by a one-tailed heteroscedastic Student's *t*-test
729 comparing the experimental value versus the appropriate negative control, is indicated by a *.

730

731 **FIG 6.** Model of localization and interactions of the ICE*Bs1* T4SS components. Cytoplasmic
732 membrane (CM) and cell wall (CW) are indicated. N-termini of proteins are indicated with an N.
733 Topology predictions were obtained as described in Figure 1 legend, and have not been
734 experimentally verified. The thick arrow indicates the interaction between ConE and ConB
735 consistent with ConE-GFP localization data and bacterial two-hybrid studies. A dotted arrow
736 indicates the possible interaction between ConE and ConD consistent with ConE-GFP
737 localization data and their genetic linkage. No other interactions have been demonstrated. In the
738 model, CwlT is drawn as a transmembrane protein and as a secreted protein since it was
739 observed both cell-associated and in culture supernatants (9). The model does not depict
740 oligomerization or interactions that have been demonstrated for other conjugative T4SSs.

741

742 **Table 1.** *B. subtilis* strains used[a]
743

| Strain | Relevant genotype or characteristics (reference) |
|---|---|
| CAL89 | ICE*Bs1*$^0$ *comK*::*spc str-84* (20) |
| CAL419 | ICE*Bs1*$^0$ *comK*::*cat str-84* (25) |
| JMA 168 | Δ(*rapIphrI*)*342*::*kan amyE*::[(Pspank(hy)-*rapI*) *spc*] (20) |
| MMB968 | Δ(*rapIphrI*)*342*::*kan amyE*::[(Pspank(hy)-*rapI*) *spc*] *lacA*::[Pxis-(*conD conE-mgfpmut2*) *tet*] (27) |
| MMB1247 | Δ(*rapIphrI*)*342*::*kan* [Δ*conQ848* (unmarked)] *amyE*::[(Pspank(hy)-*rapI*) *spc*] *lacA*::[Pxis-(*conD conE-mgfpmut2*) *tet*] |
| MMB1271 | Δ(*rapIphrI*)*342*::*kan* [*conC* Δ(*5-81*) (unmarked)] *amyE*::[(Pspank(hy)-*rapI*) *spc*] |
| MMB1273 | Δ(*rapIphrI*)*342*::*kan* [*yddF* Δ(*5-103*) (unmarked)] *amyE*::[(Pspank(hy)-*rapI*) *spc*] |
| MMB1274 | Δ(*rapIphrI*)*342*::*kan* [*conD* Δ(*5-131*) (unmarked)] *amyE*::[(Pspank(hy)-*rapI*) *spc*] |
| MMB1275 | Δ(*rapIphrI*)*342*::*kan* [*conB* Δ(*9-350*) (unmarked)] *amyE*::[(Pspank(hy)-*rapI*) *spc*] |
| MMB1283 | Δ(*rapIphrI*)*342*::*kan* [*conG* Δ(*5-805*) (unmarked)] *amyE*::[(Pspank(hy)-*rapI*) *spc*] |
| MMB1293 | Δ(*rapIphrI*)*342*::*kan* [*conC* Δ(*5-81*) (unmarked)] *amyE*::[(Pspank(hy)-*rapI*) *spc*] *lacA*::[Pxis-(*conD conE-mgfpmut2*) *tet*] |
| MMB1297 | Δ(*rapIphrI*)*342*::*kan* [*conB* Δ(*9-350*) (unmarked)] *amyE*::[(Pspank(hy)-*rapI*) |

| | |
|---|---|
| | *spc*] *lacA*::[Pxis-(*conD conE-mgfpmut2*) *tet*] |
| MMB1299 | Δ(*rapIphrI*)*342*::*kan* [*conG* Δ(*5-805*) (unmarked)] *amyE*::[(Pspank(hy)-*rapI*) *spc*] *lacA*::[Pxis-(*conD conE-mgfpmut2*) *tet*] |
| MMB1343 | Δ(*rapIphrI*)*342*::*kan* [*yddF* Δ(*5-103*) (unmarked)] *amyE*::[(Pspank(hy)-*rapI*) *spc*] *lacA*::[Pxis-(*conD conE-mgfpmut2*) *tet*] |
| MMB1390 | Δ(*rapIphrI*)*342*::*kan* [*conC* Δ(*5-81*) (unmarked)] *amyE*::[(Pspank(hy)-*rapI*) *spc*] *thrC*::[(Pspank(hy)-*conC*) *mls*] |
| MMB1393 | Δ(*rapIphrI*)*342*::*kan* [*conG* Δ(*5-805*) (unmarked)] *amyE*::[(Pspank(hy)-*rapI*) *spc*] *thrC*::[(Pspank(hy)-*conG) mls*] |
| MMB1397 | Δ(*rapIphrI*)*342*::*kan* [*conD* Δ(*5-131*) (unmarked)] *amyE*::[(Pspank(hy)-*rapI*) *spc*] *thrC*::[(Pspank(hy)-*conD) mls*] |
| MMB1412 | Δ(*rapIphrI*)*342*::*kan* [*conB* Δ(*9-350*) (unmarked)] *amyE*::[(Pspank(hy)-*rapI*) *spc*] *thrC325*::[(ICE*Bs1*-311 (Δ*attR*100::*tet*)) *mls*] |
| MMB1413 | Δ(*rapIphrI*)*342*::*kan* [*conC* Δ(*5-81*) (unmarked)] *amyE*::[(Pspank(hy)-*rapI*) *spc*] *thrC325*::[(ICE*Bs1*-311 (Δ*attR*100::*tet*)) *mls*] |
| MMB1419 | Δ(*rapIphrI*)*342*::*kan* [*conG* Δ(*5-805*) (unmarked)] *amyE*::[(Pspank(hy)-*rapI*) *spc*] *thrC325*::[(ICE*Bs1*-311 (Δ*attR*100::*tet*)) *mls*] |
| MMB1425 | ICE*Bs1*-319::*kan amyE*::[(Pspank(hy)-*rapI*) *spc*] *lacA*::[Pxis-(*conD conE-mgfpmut2*) *tet*] |
| MMB1426 | ICE*Bs1*-320::*kan amyE*::[(Pspank(hy)-*rapI*) *spc*] *lacA*::[Pxis-(*conD conE-mgfpmut2*) *tet*] |
| MMB1429 | Δ(*rapIphrI*)*342*::*kan* [*conD* Δ(*5-131*) (unmarked)] *amyE*::[(Pspank(hy)-*rapI*) |

| | |
|---|---|
| | *spc*] *thrC325*::[(ICE*Bs1*-311 (Δ*attR*100::*tet*)) *mls*] |
| MMB1473 | Δ(*rapIphrI*)*342*::*kan amyE*::[(Pspank(hy)-*rapI*) *spc*]; pBS42 *(cat)* |
| MMB1474 | Δ(*rapIphrI*)*342*::*kan* [*conB* Δ(*9-350*) (unmarked)] *amyE*::[(Pspank(hy)-*rapI*) *spc*]; pBS42 *(cat)* |
| MMB1476 | Δ(*rapIphrI*)*342*::*kan* [*conC* Δ(*5-81*) (unmarked)] *amyE*::[(Pspank(hy)-*rapI*) *spc*]; pBS42 *(cat)* |
| MMB1477 | Δ(*rapIphrI*)*342*::*kan* [*conC* Δ(*5-81*) (unmarked)] *amyE*::[(Pspank(hy)-*rapI*) *spc*] *thrC*::[(Pspank(hy)-*conC) mls*]; pBS42 *(cat)* |
| MMB1478 | Δ(*rapIphrI*)*342*::*kan* [*conD* Δ(*5-131*) (unmarked)] *amyE*::[(Pspank(hy)-*rapI*) *spc*]; pBS42 *(cat)* |
| MMB1479 | Δ(*rapIphrI*)*342*::*kan* [*conD* Δ(*5-131*) (unmarked)] *amyE*::[(Pspank(hy)-*rapI*) *spc*] *thrC*::[(Pspank(hy)-*conD) mls*]; pBS42 *(cat)* |
| MMB1480 | Δ(*rapIphrI*)*342*::*kan* [*conE* (*K476E*) (unmarked)] *amyE*::[(Pspank(hy)-*rapI*) *spc*]; pBS42 *(cat)* |
| MMB1481 | Δ(*rapIphrI*)*342*::*kan* [*conE* (*K476E*) (unmarked)] *amyE*::[(Pspank(hy)-*rapI*) *spc*] *thrC*::[(Pxis-(*conD conE-lacZ)) mls*]; pBS42 *(cat)* |
| MMB1482 | Δ(*rapIphrI*)*342*::*kan* [*yddF* Δ(*5-103*) (unmarked)] *amyE*::[(Pspank(hy)-*rapI*) *spc*]; pBS42 *(cat)* |
| MMB1483 | Δ(*rapIphrI*)*342*::*kan* [*yddF* Δ(*5-103*) (unmarked)] *amyE*::[(Pspank(hy)-*rapI*) *spc*] *thrC*::[(Pspank(hy)-*yddF) mls*]; pBS42 *(cat)* |
| MMB1484 | Δ(*rapIphrI*)*342*::*kan* [*conG* Δ(*5-805*) (unmarked)] *amyE*::[(Pspank(hy)-*rapI*) *spc*]; pBS42 *(cat)* |

| | |
|---|---|
| MMB1485 | Δ(*rapIphrI*)*342*::*kan* [*conG* Δ(*5-805*) (unmarked)] *amyE*::[(Pspank(hy)-*rapI*) *spc*] *thrC*::[(Pspank(hy)-*conG) mls*]; pBS42 *(cat)* |
| MMB1547 | Δ(*rapIphrI*)::*cat amyE*::[(Pspank(hy)-*rapI*) *spc*] *conE*::pMMB1530 (*conE-mgfpmut2 kan*) |
| MMB1548 | Δ(*rapIphrI*)::*cat* [*conC* Δ(*5-81*) (unmarked)] *amyE*::[(Pspank(hy)-*rapI*) *spc*] *conE*::pMMB1530 (*conE-mgfpmut2 kan*) |
| MMB1549 | Δ(*rapIphrI*)::*cat* [*conD* Δ(*5-131*) (unmarked)] *amyE*::[(Pspank(hy)-*rapI*) *spc*] *conE*::pMMB1530 (*conE-mgfpmut2 kan*) |
| MMB1550 | Δ(*rapIphrI*)::*cat* [*conB* Δ(*9-350*) (unmarked)] *amyE*::[(Pspank(hy)-*rapI*) *spc*] *conE*::pMMB1530 (*conE-mgfpmut2 kan*) |
| MMB1715 | ICE*Bs1*$^{0}$ *thrC*::[(Pspank(hy)-(*conB conC conD conE-mgfpmut2*) *mls*] |
| MMB1735 | Δ(*rapIphrI*)*342*::*kan* [*conB* Δ(*9-350*) (unmarked)] *amyE*::[(Pspank(hy)-*rapI*) *spc*] *thrC*::[(Pspank(hy)-*conB) mls*] |
| MMB1760 | Δ(*rapIphrI*)*342*::*kan* [*conB* Δ(*9-350*) (unmarked)] *amyE*::[(Pspank(hy)-*rapI*) *spc*] *thrC*::[(Pspank(hy)-*conB) mls*]; pBS42 (*cat*) |
| MMB1763 | Δ(*rapIphrI*)*342*::*kan* [*conB* Δ(*9-350*) (unmarked)] *amyE*::[(Pspank(hy)-*rapI*) *spc*] *lacA*:: [Pxis-(*conD conE-mgfpmut2*) *tet*] *thrC1755*::[ICE*Bs1* (Δ*conC-attR*::*cat*) *mls*] |
| MMB1764 | Δ(*rapIphrI*)*342*::*kan* [*conB* Δ(*9-350*) (unmarked)] *amyE*::[(Pspank(hy)-*rapI*) *spc*] *lacA*::[Pxis-(*conD conE-mgfpmut2*) *tet*] *thrC1756*::[ICE*Bs1* (Δ*conB-attR*::*cat*) *mls*] |

744 [a] All strains are derived from JH642 (31) and contain *pheA1* and *trpC2.*

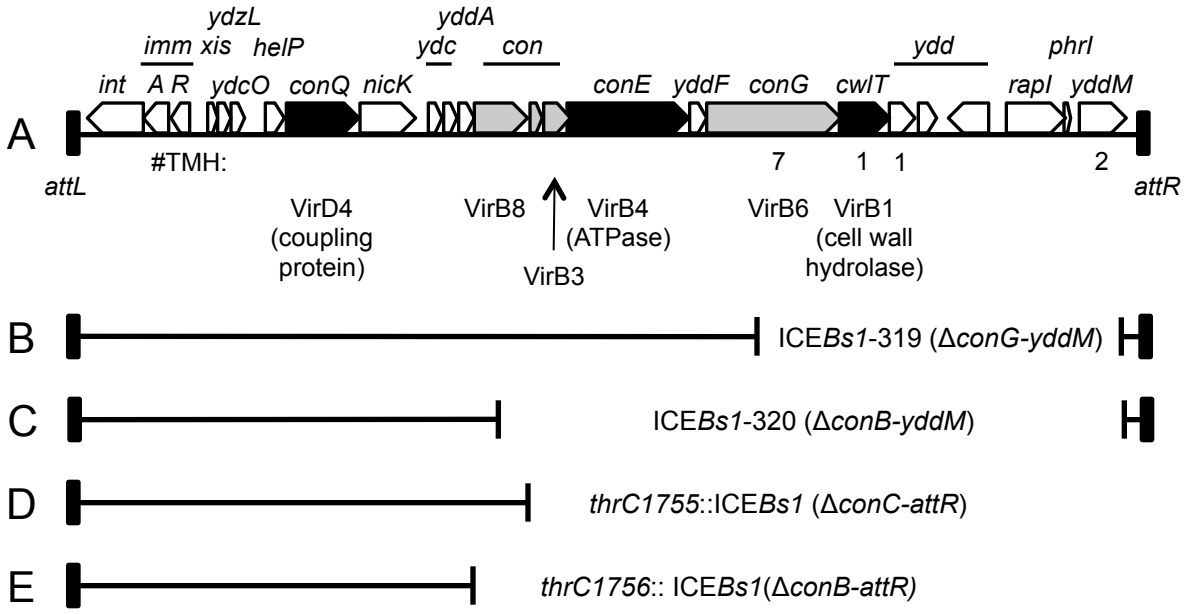
A
ydzL
imm
xis
helP
yddA
ydc
con
ydd
phrI
int
A
R
ydcO
conQ
nicK
conE
yddF
conG
cwlT
rapI
yddM
#TMH:
7
1
1
2
attL
attR
VirD4
(coupling
protein)
VirB8
VirB4
(ATPase)
VirB3
VirB6
VirB1
(cell wall
hydrolase)
B
ICEBs1-319 (ΔconG-yddM)
C
ICEBs1-320 (ΔconB-yddM)
D
thrC1755::ICEBs1 (ΔconC-attR)
E
thrC1756:: ICEBs1(ΔconB-attR)

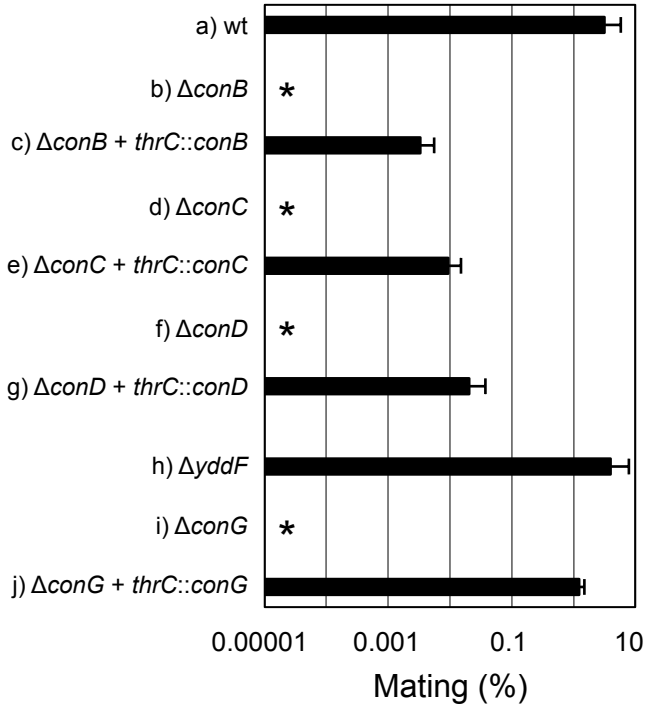
a) wt
b) Δ*conB*
c) Δ*conB* + *thrC*::*conB*
d) Δ*conC*
e) Δ*conC* + *thrC*::*conC*
f) Δ*conD*
g) Δ*conD* + *thrC*::*conD*
h) Δ*yddF*
i) Δ*conG*
j) Δ*conG* + *thrC*::*conG*
*
*
*
*
0.00001
0.001
0.1
10
Mating (%)

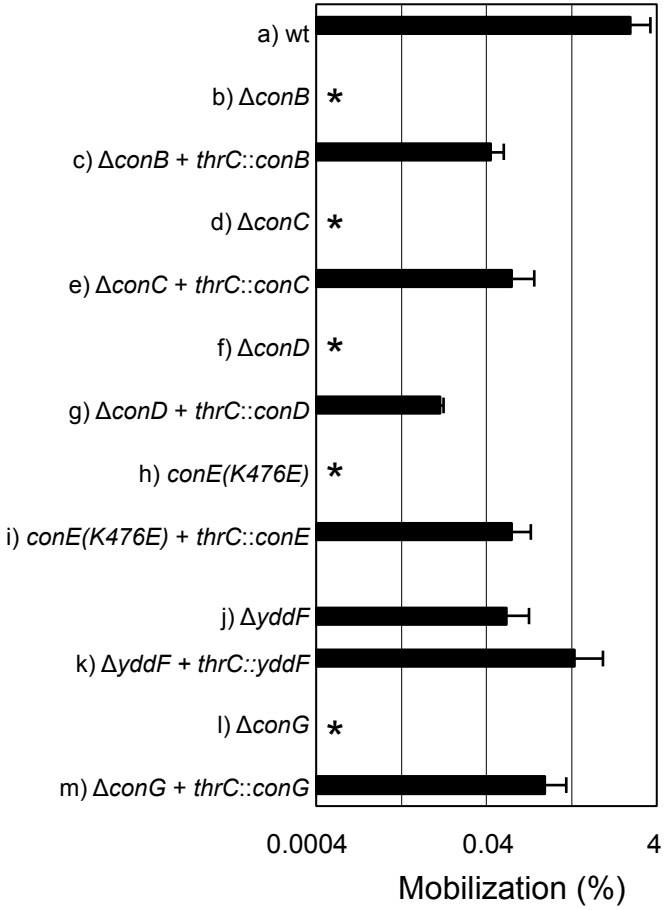
a) wt
b) ΔconB
c) ΔconB + thrC::conB
d) ΔconC
e) ΔconC + thrC::conC
f) ΔconD
g) ΔconD + thrC::conD
h) conE(K476E)
i) conE(K476E) + thrC::conE
j) ΔyddF
k) ΔyddF + thrC::yddF
l) ΔconG
m) ΔconG + thrC::conG
*
0.0004
0.04
4
Mobilization (%)

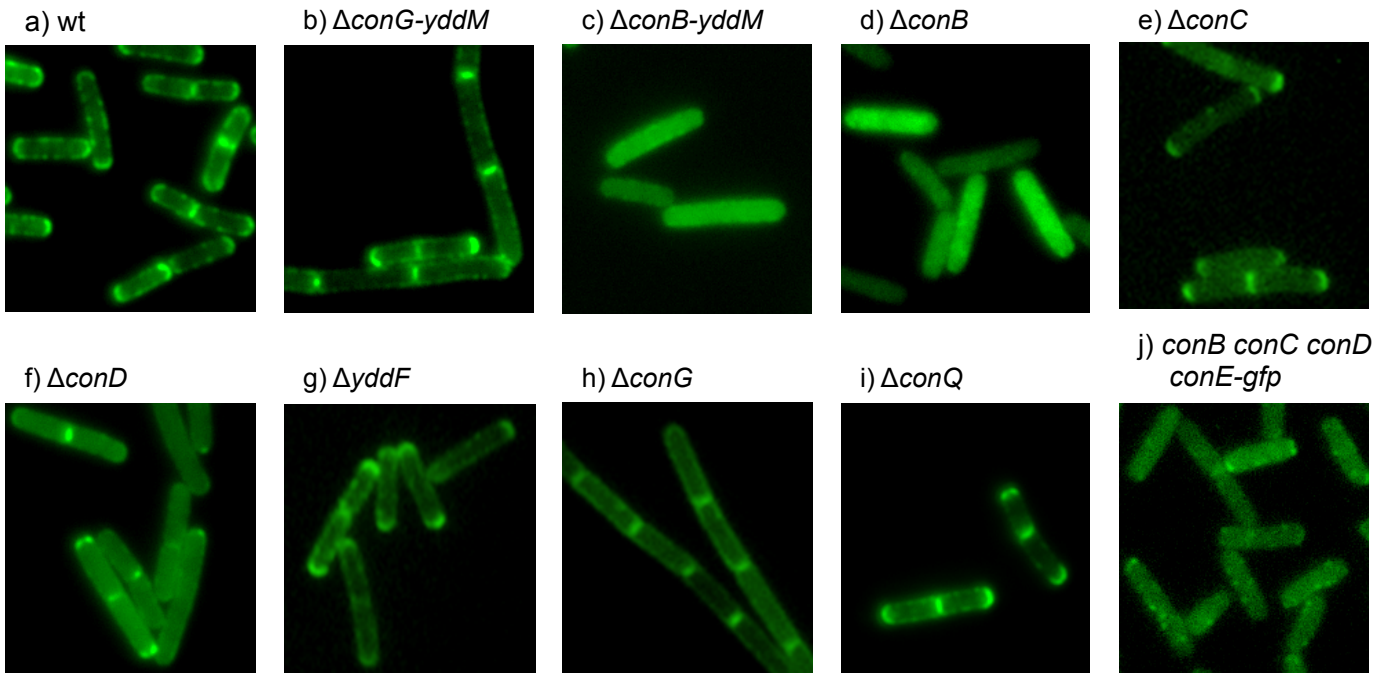
a) wt
b) Δ*conG-yddM*
c) Δ*conB-yddM*
d) Δ*conB*
e) Δ*conC*
f) Δ*conD*
g) Δ*yddF*
h) Δ*conG*
i) Δ*conQ*
j) *conB conC conD conE-gfp*

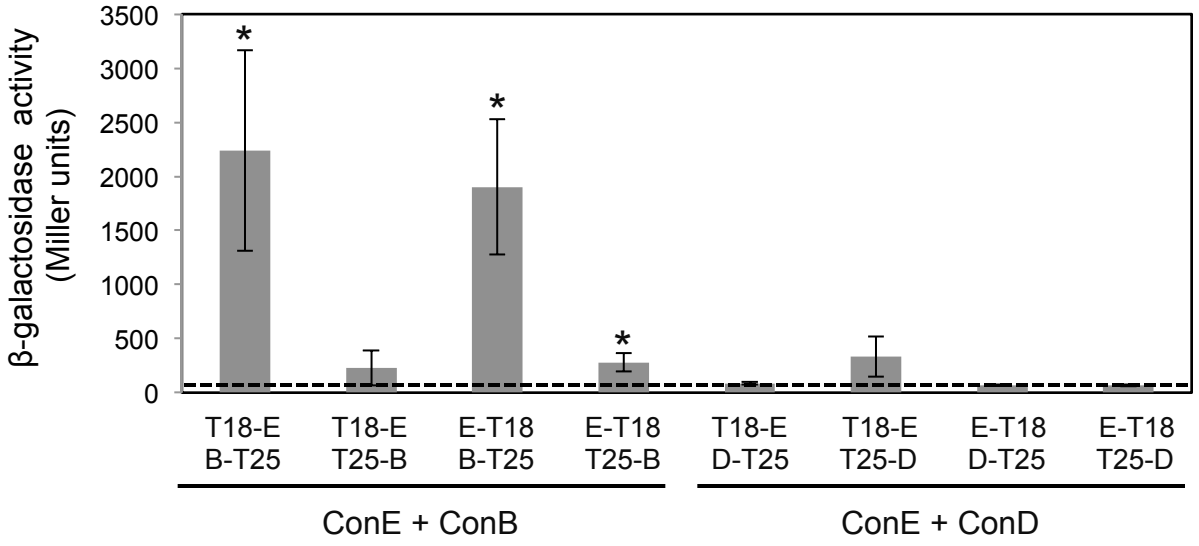
β-galactosidase activity
(Miller units)
3500
3000
2500
2000
1500
1000
500
0
*
*
*
T18-E
B-T25
T18-E
T25-B
E-T18
B-T25
E-T18
T25-B
T18-E
D-T25
T18-E
T25-D
E-T18
D-T25
E-T18
T25-D
ConE + ConB
ConE + ConD

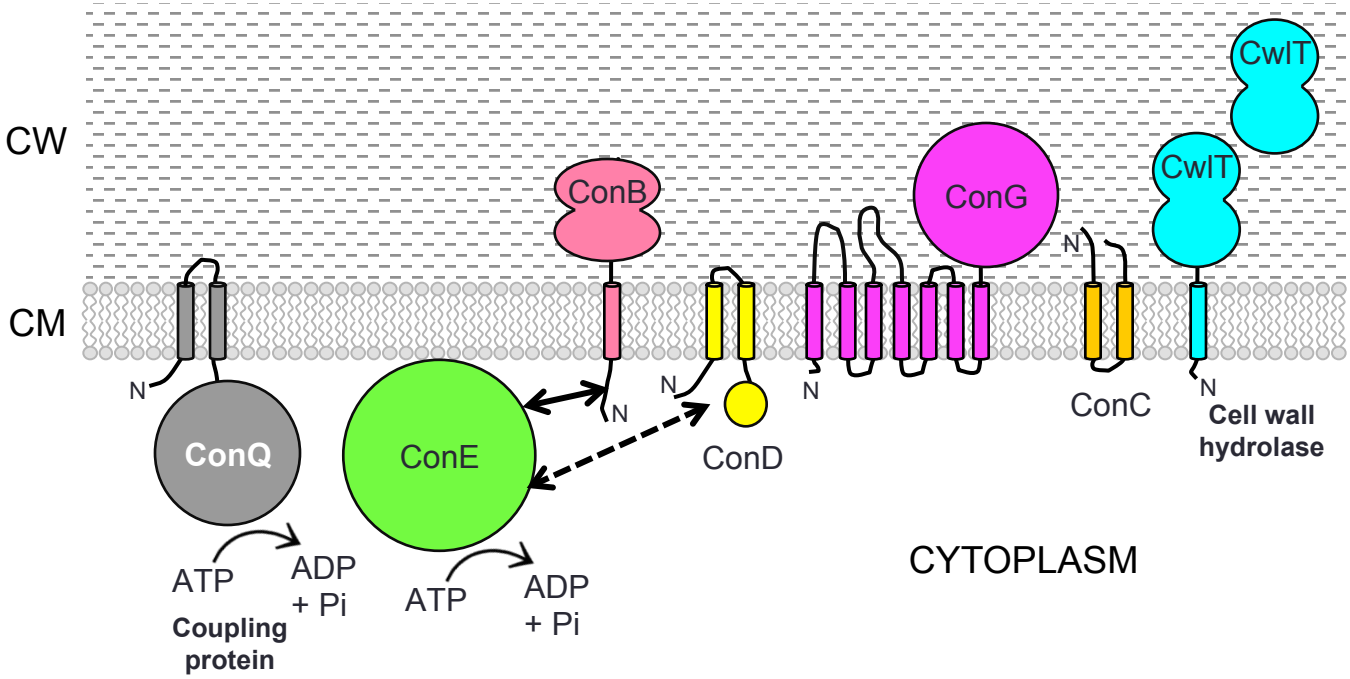
CW
CM
CwlT
CwlT
ConB
ConG
N
N
N
N
N
ConC
Cell wall
hydrolase
ConQ
ConE
ConD
ATP
ADP
+ Pi
Coupling
protein
ATP
ADP
+ Pi
CYTOPLASM